Science of the Total Environment 572 (2016) 119–128

Contents lists available at ScienceDirect

Science of the Total Environment

journal homepage: www.elsevier.com/locate/scitotenv

Alpine vegetation phenology dynamic over 16 years and its covariation with climate in a semi-arid region of China

Jihua Zhou [a,b], Wentao Cai [a,b], Yue Qin [c], Liming Lai [a], Tianyu Guan [a,b], Xiaolong Zhang [a,b], Lianhe Jiang [a], Hui Du [a], Dawen Yang [c], Zhentao Cong [c], Yuanrun Zheng [a,*]

[a] Key Laboratory of Resource Plants, Beijing Botanical Garden, West China Subalpine Botanical Garden, Institute of Botany, Chinese Academy of Sciences, Xiangshan, Beijing, 100093, China
[b] University of Chinese Academy of Sciences, Beijing 100049, China
[c] State Key Laboratory of Hydro-science and Engineering, Department of Hydraulic Engineering, Tsinghua University, Beijing 100084, China

HIGHLIGHTS

- alpine vegetation phenology dynamics is crucial to climatic warming.
- The maximum NDVI in five vegetation groups increased significantly in study period.
- The start of growing season, growing season length, maximum NDVI were significantly correlated with temperature.
- The maximum NDVI was significantly correlated with grazing productions.

GRAPHICAL ABSTRACT

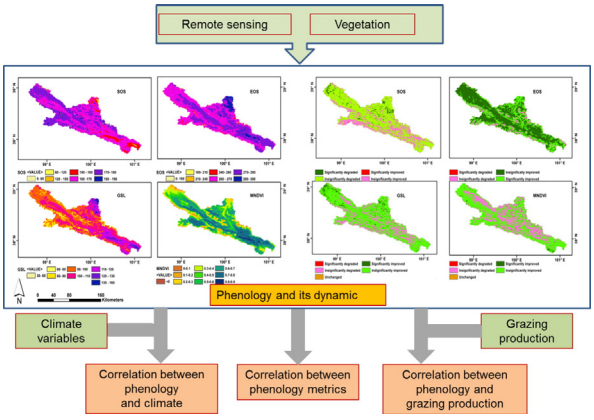

ARTICLE INFO

Article history:
Received 13 June 2016
Received in revised form 27 July 2016
Accepted 29 July 2016
Available online xxxx

Editor: P Elena Paoletti

Keywords:
Heihe River
Phenology
Remote sensing
Alpine vegetation
Normalized Difference Vegetation Index
Climate variability

ABSTRACT

Vegetation phenology is a sensitive indicator of ecosystem response to climate change, and plays an important role in the terrestrial biosphere. Improving our understanding of alpine vegetation phenology dynamics and the correlation with climate and grazing is crucial for high mountains in arid areas subject to climatic warming. Using a time series of SPOT Normalized Difference Vegetation Index (NDVI) data from 1998 to 2013, the start of the growing season (SOS), end of the growing season (EOS), growing season length (GSL), and maximum NDVI (MNDVI) were extracted using a threshold-based method for six vegetation groups in the Heihe River headwaters. Spatial and temporal patterns of SOS, EOS, GSL, MNDVI, and correlations with climatic factors and livestock production were analyzed. The MNDVI increased significantly in 58% of the study region, whereas SOS, EOS, and GSL changed significantly in <5% of the region. The MNDVI in five vegetation groups increased significantly by a range from 0.045 to 0.075. No significant correlation between SOS and EOS was observed in any vegetation group. The SOS and GSL were highly correlated with temperature in May and April–May, whereas MNDVI was correlated with temperature in August and July–August. The EOS of different vegetation groups was correlated with different climatic variables. Maximum and minimum temperature, accumulated temperature, and effective accumulated temperature showed stronger correlations with phenological metrics compared with those of

* Correspondence author at: Key Laboratory of Plant Resources, Institute of Botany, Chinese Academy of Sciences, No. 20 Nanxincun, Xiangshan, Beijing 100093, China.
E-mail address: zhengyr@ibcas.ac.cn (Y. Zheng).

http://dx.doi.org/10.1016/j.scitotenv.2016.07.206

mean temperature, and should receive greater attention in phenology modeling in the future. Meat and milk production were significantly correlated with the MNDVI of scrub, steppe, and meadow. Although the MNDVI increased in recent years, ongoing monitoring for rangeland degradation is recommended.

1. Introduction

Vegetation phenology is a sensitive indicator of ecosystem response to climate change and plays an important role in ecosystem carbon and hydrological cycles (Pau et al., 2011; Richardson et al., 2013). Phenology varies greatly over broad geographic gradients, according to climate zone and vegetation type, and shows substantial inter-annual variability in the start of the growing season (SOS), the end of the growing season (EOS), and growing season length (GSL), which is a result of year-to-year variability in weather (Richardson et al., 2013). Dramatic climate change in recent decades has been confirmed in several studies and has resulted in phenological changes in many biomes, especially in temperate and boreal regions (Menzel and Fabian, 1999; Penuelas et al., 2009; Sun et al., 2015). Altered phenology will in turn feedback to climate through changes in biogeochemical cycling and biophysical properties (e.g., albedo) (Bonan, 2008; Fu et al., 2015). Therefore, understanding phenological variation is critical to improve terrestrial biosphere models and climate models (Richardson et al., 2012; Jin et al., 2013).

At middle and high latitudes, phenology is controlled by temperature, winter chilling, and photoperiod, but at a regional scale, water limitations may also be important (Jolly et al., 2005; Koerner and Basler, 2010; Richardson et al., 2013). Numerous studies have documented advances in spring phenology coupled with patterns of temperature in boreal ecosystems and arctic tundra (He et al., 2015). Environmental drivers, such as temperature, photoperiod, and water and nutrient availability, regulate the SOS of natural vegetation (Xin et al., 2015), and changes in the timing of autumn phenology in response to climate change are less well documented than changes in spring phenology. Some studies have reported delays in EOS, and these trends have been linked to increases in late summer or early autumn temperatures (Richardson et al., 2013). However, our understanding of mechanistic phenology processes remains limited (Richardson et al., 2013; Jin and Eklundh, 2014).

Ground observations, mathematical models, and satellite observations are the main methods used in the study of large-scale phenological patterns (Jolly et al., 2005). Most phenological observations have focused on cultivated plants rather than natural vegetation at the local level (Fu et al., 2014). In addition, warming, cutting, and transplant experiments offer novel perspectives for phenological studies, especially for mechanistic investigations (Wolkovich et al., 2012). Although modeling of spring vegetation phenology via climatic variables has received extensive attention recently at different scales (Xin et al., 2015), remote sensing is often used for large-scale spatial and temporal phenological studies (Zhao et al., 2012). Many studies that used in situ measurements and satellite observations have documented decadal shifts in vegetation phenology under a changing climate at both regional and global scales. PhenoCams is a promising method to help bridge the gap between satellite monitoring and traditional on-the-ground observations (Richardson et al., 2013; Brown et al., 2016).

Many phenological studies have focused on temperate and boreal ecosystems, whereas few have studied alpine vegetation (Ge et al., 2015), which represents a more severe habitat and is more sensitive to climate change (Zhang et al., 2013; Shen et al., 2014). Several studies have investigated vegetation phenology on the Tibetan Plateau (Jin et al., 2013; Zhang et al., 2013; Shen et al., 2015b) or a single vegetation type (Du et al., 2014; Wang et al., 2014; Zhou et al., 2014; He et al., 2015), but not in a river basin located in an arid area with highly complex terrain and, in particular, desert and sparse alpine vegetation have not been studied. Alpine vegetation in arid areas is even more complex than that in wetter regions because vegetation groups range from desert in the lower reaches to glaciers in the upper reaches. Understanding vegetation phenology using a reasonable method is essential, especially in remote and undeveloped areas (Cheng et al., 2014).

The Qilian Mountains in northwestern China is an ecotone of the Tibetan Plateau, the Loess Plateau, the Central Asian deserts, and the Qaidam Desert (Cheng et al., 2014). The vegetation is typical of alpine vegetation located in an arid area, and many vegetation types are distributed at different elevations and habitats, including forest, scrub, grassland, meadow, and desert. The phenology and the response to climate changes among the different vegetation types are likely to differ. Grazing is the main land use in the Qilian Mountains. The vegetation phenology affects the livelihoods of residents because their traditional nomadic lifestyle may be adversely affected when livestock experience poor grazing owing to a lack of forage in spring when the green-up onset is delayed (Shen et al., 2014; Wang et al., 2016a) or the growing season is changed (Keenan and Richardson, 2015; Wu et al., 2016). However, the vegetation phenology dynamics in the Qilian Mountains are unknown (Shen et al., 2014; Wang et al., 2016a).

In this study, Satellites Pour l'Observation de la Terre (SPOT) vegetation data were used to quantify the vegetation phenology in the Qilian Mountains in an arid area and to assess the correlation with climatic variation and human activities. The objectives were to (1) analyze the spatial and temporal patterns of phenological metrics of alpine vegetation in an arid area, (2) evaluate the inter-annual relationship between phenological metrics and climatic variation for alpine vegetation, and (3) evaluate the inter-annual relationship between grazing products and phenological events for alpine vegetation.

2. Materials and methods

2.1. Study area and vegetation

The headwaters of the Heihe River Basin are located in the middle section of the Qilian Mountains, which range from 98°34′ to 101°11′E and 37°41′ to 39°05′N (Fig. 1) and cover an area of approximately 10,009 km^2. The Qilian Mountains lie to the north of the Tibet Plateau and to the south of the Hexi Corridor (Silk Road). Elevation ranges from 1668 to 5062 m (calculated from ASTER GDEM, http://westdc.westgis.ac.cn/). The annual precipitation is between 149 and 486 mm and shows high seasonal variability, with nearly 60% of the total annual rainfall concentrated in summer from June to September. The mean annual temperature ranges from −9.8 to 6.9 °C, with cooler average temperatures recorded with increasing elevation. Precipitation decreases from east to west and increases from north to south in the study area, whereas temperature shows the reverse pattern (Cheng et al., 2014; Gao et al., 2016).

The Vegetation Map of the People's Republic of China (VMC, 1:1,000,000) (Editorial Committee of Vegetation Map of China, CAS, 2007) depicts the Qilian Mountains as containing seven vegetation groups (see Table 1 and Fig. 2). The lowlands (1600–2400 m) are mainly desert and the middle altitudes (2400–2800 m) are steppe, with needleleaf forest in the north ranging from 2400 to 3200 m, scrub and meadow from 3200 to 4000 m, and alpine vegetation in areas higher than 4000 m. Glaciers are present on some peaks in the Qilian Mountains. The main land use is grazing. The forest is formally protected in nature conservation reserves and logging has been prohibited in recent years (Qinghai Bureau of Statistics, 1998–2014). Agricultural and horticultural crops is grown near counties and towns and covers an area of

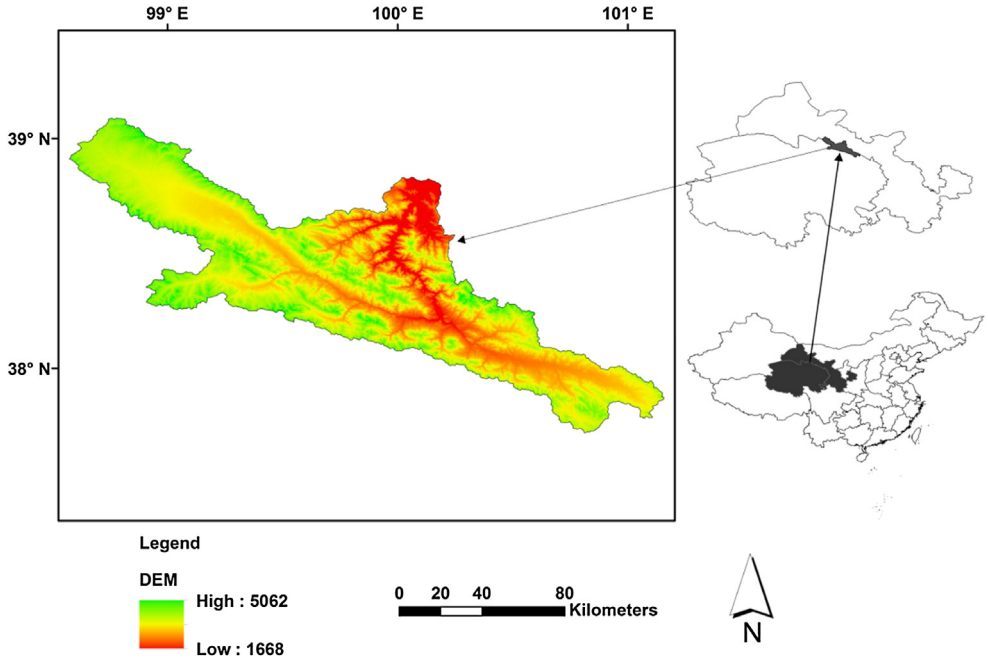

Fig. 1. Location and elevation of the study area.

<1% of the study region. This study focused on natural vegetation, and specifically we chose needleleaf forest, scrub, desert, steppe, meadow, and alpine vegetation for analysis. Vegetation information was derived from the VMC. The original electronic vector map was converted to a 1 km × 1 km raster version using the Polygon to Raster tool in ArcGIS 10.0. We used field survey data, Landsat8 images, and Google Earth to locate typical vegetation groups in the study region. We extracted 36–50 points for each vegetation group to further analyze their phenology and the correlations with climatic parameters. The samples were extracted by typical vegetation points and were as much as possible evenly distributed in each vegetation type of each vegetation group. Therefore, from the selected vegetation points, >90% of the target vegetation was covered.

2.2. Climate data sets and land use

The climate data used in this study consisted of monthly maximum, minimum, and mean temperatures and monthly precipitation. The gridded temperature data were interpolated from the meteorological stations using the inverse-distance weighting method and adjusted in accordance with elevation (Yang et al., 2004). The gridded precipitation data were interpolated using the method of Shen and Xiong (2016). The data set had a spatial resolution of 1 km. The gridded climate data were downloaded from the Cold and Arid Regions Science Data Center at Lanzhou (http://westdc.westgis.ac.cn) (Gao et al., 2016). Annual mean climate data were also calculated.

The main land use of the headwaters of the Heihe River Basin is grazing, and the headwaters are mostly within Qilian County. Therefore, grazing data for Qilian County were used to represent grazing in the headwaters of the Heihe River Basin. Cold temperatures and frequent snowstorms in winter and spring are permanent threats to herder communities, and snowstorms lead to a high livestock mortality rate in some years (Wang et al., 2016a). In the 1980s, livestock and pastures were mostly allocated to individual herder households. In 1998, 80% of the total area of winter and spring pasture was fenced in Qilian County. From 2003 to 2005, pastures involved in the "Grain to Green" program were abandoned as natural grasslands. After 2004, rotational grazing has implemented in Qilian County, and consequently a large number of warm houses for cattle were built funded by government subsidies (Qinghai Bureau of Statistics, 1998–2014). Data on meat and milk production, which we considered to be indicators of grazing intensity, were acquired from the Qinghai Economic Yearbook (Qinghai Bureau of Statistics, 1998–2014).

Table 1
Description of vegetation groups in the Heihe River headwaters.

Vegetation group	Description
1. Needleleaf forest	Temperate and temperate-montane needleleaf forest with dominant species *Picea crassifolia*.
2. Scrub	Subalpine broadleaf deciduous scrub with dominant species *Salix gilashania*, *S. oritrepha*, *S. oritrepha*, *Dasiphora fruticosa*.
3. Desert	Temperate semi-shrubby and dwarf semi-shrubby desert with dominant species *Sympegma regelii*.
4. Steppe	Temperate needlegrass arid steppe, alpine grassland and *Carex* steppe with dominant species *Stipa krylovii*, *S. penicillata*, *S. breviflora*, *S. bungeana*, *S. purpurea*.
5. Meadow	Alpine *Kobresia* spp., forb meadow with dominant species *Kobresia pygmaea*, *K. humilis*, *K. filifolia*, *K. schoenoides*, *Carex* spp., *Elymus nutans*, *Roegneria nutans*.
6. Alpine vegetation	Alpine sparse vegetation with dominant species *Saussurea medusa*, *S.* spp., *Rhodiola rosea*, *Cremanthodium* spp.
7. Culture vegetation	One annual, short growing period, cold-resistant crop with dominant species spring barley, spring wheat, potato, turnip, pea, rapeseed.
8. Land without vegetation	Predominantly glaciers and permanent snow beds.

2.3. Remote sensing and phenology algorithm

The SPOT (http://www.vgt.vito.be/) Normalized Difference Vegetation Index (NDVI) data were used to determine phenological metrics in the headwaters of the Heihe River Basin. The data used were 1-km resolution 10-day composite data (S10) in the Plate-Carrée projection for the years 1998–2013. Data for 1998 began on April 1, as the SOS of the headwaters of the Heihe Biver basin is early May; therefore the data for 1998 covered a full growing season. The data have already been systematically corrected for the effects of atmosphere and terrain (Maisongrande et al., 2004). Time-series NDVI data were smoothed using the Savitzky–Golay filter (Jonsson and Eklundh, 2004). The filter employs vegetation index time-series characterizations to smooth out

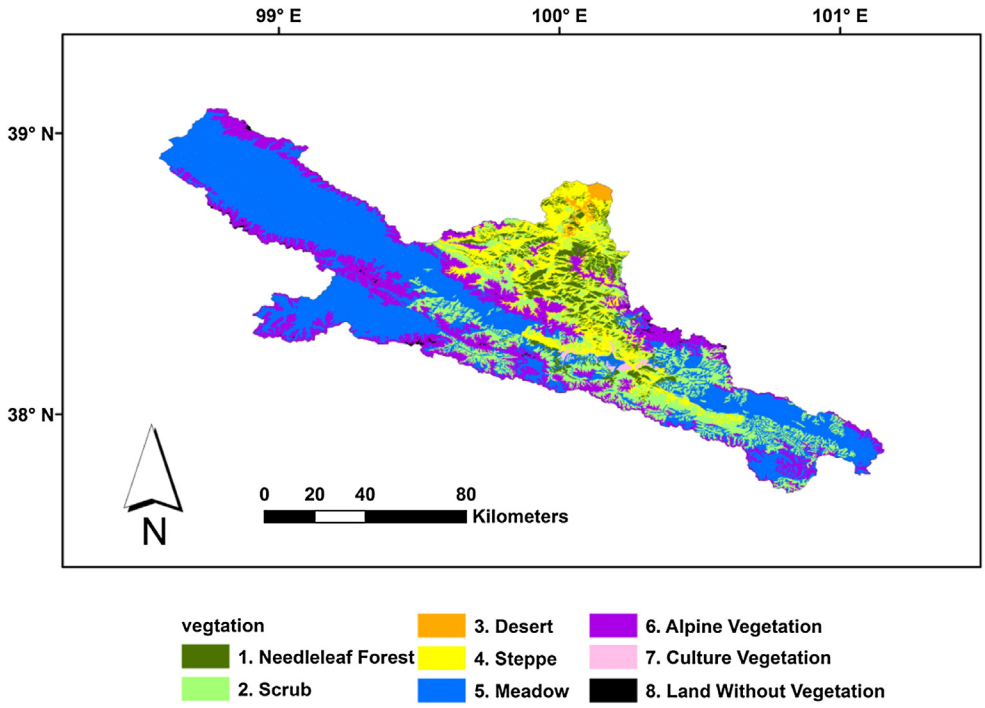

Fig. 2. Vegetation groups in the study area. Description of the vegetation groups is presented in Table 1.

the noise caused by clouds or poor atmospheric conditions, and is a stable method for the extraction of phenological parameters (Lara and Gandini, 2016). The SOS and EOS were determined by the relative threshold method from the NDVI time series (Jonsson and Eklundh, 2004; He et al., 2015). The dates of SOS or EOS were defined as the times at which NDVI values increased (SOS) or decreased (EOS) to a certain proportion of the seasonal amplitude in the left or the right edge of the annual curve. A relative threshold of 0.5 was used based on previous suggestions and results obtained in similar environments (Du et al., 2014; He et al., 2015). The GSL was calculated as the difference between EOS and SOS (Wu et al., 2016). The maximum NDVI was extracted from the smoothed NDVI curve. The analysis was performed with TIMESAT 3.2 software (http://web.nateko.lu.se/timesat/timesat.asp) (Shen et al., 2015a; Wu et al., 2016).

2.4. Statistical analyses

The Mann–Kendall test (Hamed, 2008) and the Theil–Sen median slope estimator (Akritas et al., 1995) were used to determine possible monotonic trends in the time series of the phenological metrics and maximum NDVI (MNDVI) at the pixel level. These statistical procedures are widely used to determine variations in vegetation (Wang et al., 2016b). The Mann–Kendall test is a robust non-parametric significance test, and $t < 0.05$ was defined as statistically significant (Hamed, 2008). The Theil–Sen median slope estimator (Akritas et al., 1995) is a robust simple linear regression that selects the median slope calculated between any pair of data points in a time series, and hence compensates for the Mann–Kendall test in a quantitative context. This method is appropriate for assessing the rate of change in short or noisy time series because it is robust to outliers. We classified phenological metrics into five categories, namely "significantly degraded", "insignificantly degraded", "unchanged", "insignificantly improved", and "significantly improved", on the basis of the Mann–Kendall and Theil–Sen estimates. A Theil–Sen value greater than zero, equal to zero, or less than zero was defined as "improved", "unchanged", and "degraded", respectively. A significant change was based on the Mann–Kendall test value. We also used average values instead of pixel values to investigate linear trends in the phenological metrics for the six vegetation groups.

Average values for each vegetation group were used to investigate the relationship between phenological metrics and climatic variables (Du et al., 2014; Zhao et al., 2012). We used three categories of climatic variables: precipitation, temperature, and integrated index. In addition to the afore-mentioned temperature variables (see Section 2.2), the accumulated temperature (AT) and effective accumulated temperature (EAT) over 0, 2, 5, and 10 °C were calculated (Shen et al., 2015a; Xin et al., 2015). The integrated index included the Kira index (KI; Kira, 1991), Holdridge potential evapotranspiration ratio (HR; Leslie, 1967), and de Martonne aridity index (MI; Botzan et al., 1998), which are suitable indices for characterizing the physical environment of China (Meng et al., 2004). The individual indices were calculated with the following formulae:

$$\mathrm{MI} = \frac{P}{T+10}, \tag{1}$$

where P is annual precipitation and T is mean annual temperature.

$$\mathrm{WI} = \sum (t-5), \tag{2}$$

$$\mathrm{KI} = \frac{P}{\mathrm{WI}+20}, \tag{3}$$

$$\mathrm{KI} = \frac{2P}{\mathrm{WI}+140}, \tag{4}$$

where WI is the warmth index and t is the monthly mean temperature >5 °C, when $WI > 100$ Eq. (4) was used, otherwise Eq. (3) was used to calculate KI.

$$\mathrm{ABT} = \frac{1}{12}\sum t_i, \tag{5}$$

$$\mathrm{PE} = 58.93 \times \mathrm{ABT}, \tag{6}$$

$$\mathrm{PER} = \frac{\mathrm{PE}}{P}, \tag{7}$$

where *ABT* is the annual biotemperature, t_i is the temperature between 0 °C and 30 °C, when t_i is outside the extent, the edge value (0 °C or 30 °C) is used, *PE* is potential evapotranspiration, *PER* is the potential evapotranspiration ratio, and *P* is annual precipitation. To choose appropriate timescales for the phenological metrics and climatic variables, different periods were selected for the analysis: for SOS, winter (November to March), April, May, June, and April–May climatic variables were used; for EOS and GSL, winter (November to March), April, May, June, April–May, June, July, September, October, and June–July climatic variables were used; for MNDVI, winter (November to March), April, May, June, April–May, June, July, and June–July climatic variables were used; and annual mean climatic variables were also used for each phenological metric. The correlation coefficient (r) and p-values were calculated to determine the significance of the relationship (Wu et al., 2016).

Interaction effects between SOS and EOS were calculated to determine if the two parameters are correlated in the headwaters of the Heihe River Basin. The relationship between phenological metrics and grazing productivity parameters was calculated for scrub, steppe, and meadow, which are the main vegetation groups used for grazing in the study area. The correlation coefficient (r) and p-values were calculated to determine the significance of the relationship.

3. Results

3.1. Spatial and temporal variation in phenological metrics

The SOS was mostly on days of year (DOY) 150–180, the EOS was mostly on DOY 260–280, and the GSL was 80–130 days (Fig. 3). The distribution of MNDVI was associated with elevation and vegetation group. For SOS, EOS, and GSL, <5% of the study region changed significantly over the study period (Table 2, Fig. 4). In contrast, >90% of the study region showed improved MNDVI, and >58% of the region showed significantly improved MNDVI (Table 2, Fig. 4).

3.2. Phenology dynamics

The MNDVI showed a significant positive correlation with needleleaf forest ($r = 0.696$, $p = 0.003$), scrub ($r = 0.750$, $p = 0.001$), desert ($r = 0.562$, $p = 0.023$), steppe ($r = 0.647$, $p = 0.007$), and meadow ($r = 0.824$, $p < 0.001$), whereas the other phenological metrics examined did not change significantly. Although the changes in SOS, EOS, and GSL were not significant in the study period, fluctuation in the DOY was apparent. The difference of years were >20 days for SOS and GSL, >10 days for EOS, and desert showed a greater variation than the other vegetation groups (Appendices, Figs. A.1–A. 3, Fig. 5).

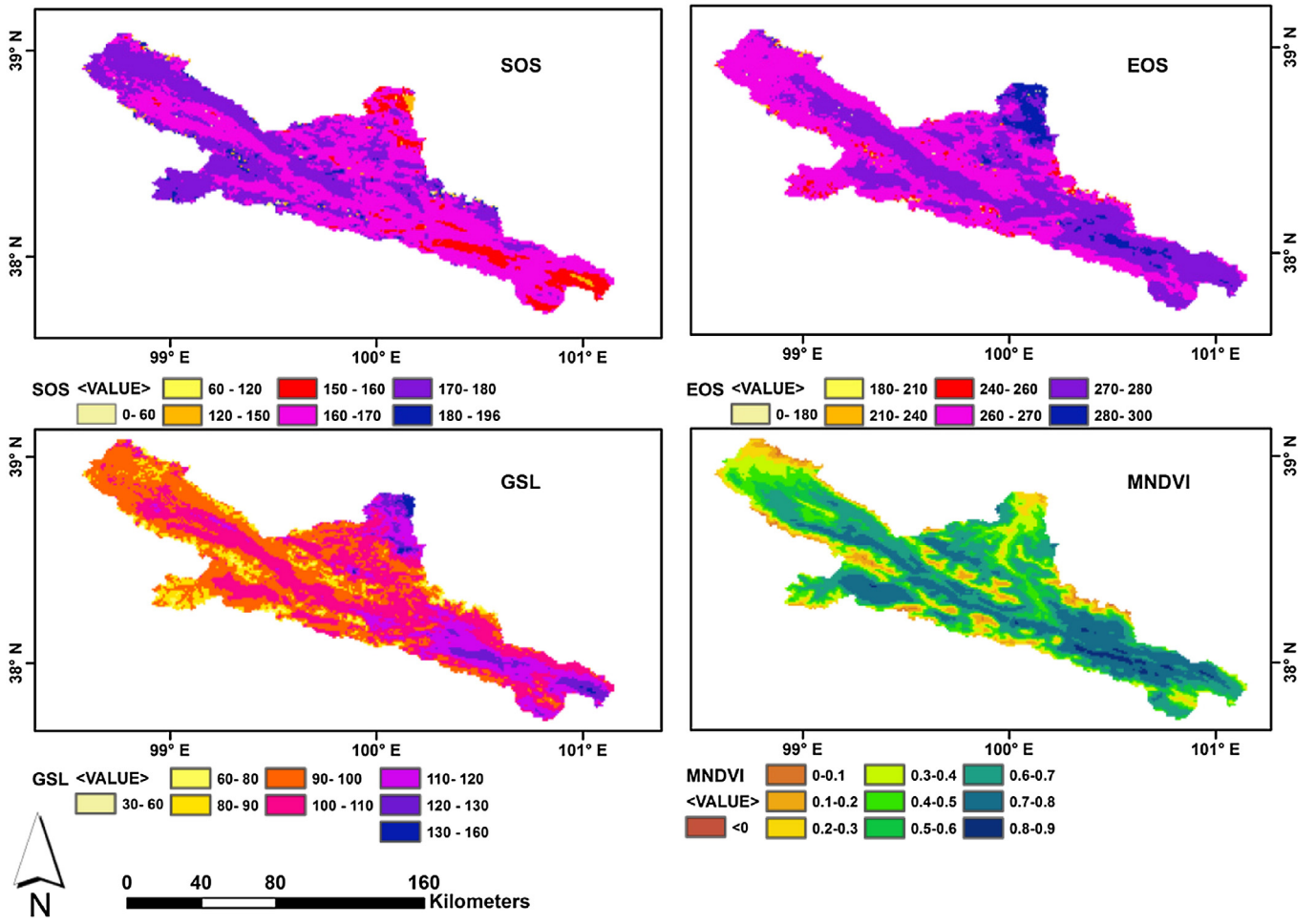

Fig. 3. Spatial pattern of 16-year average forest phenology at the start of the growing season (SOS), end of the growing season (EOS), growing season length (GSL) and maximum normalized difference vegetation index (MNDVI) in the Heihe River headwaters.

Table 2
Pixel-based nonparametric phenology trend analysis in the Heihe River headwaters. Abbreviations: Start of the growing season, SOS; end of the growing season, EOS; growing season length, GSL; maximum normalized difference vegetation index, MNDVI.

	Significantly improved	Insignificantly improved	Unchanged	Significantly degraded	Insignificantly degraded
SOS	0.15%	25.73%	0.00%	69.55%	4.56%
EOS	1.49%	60.48%	0.00%	37.76%	0.27%
GSL	4.48%	70.34%	0.08%	25.03%	0.06%
MNDVI	58.23%	34.02%	0.06%	7.47%	0.22%

3.3. Relationship between different phenological indices

The SOS and EOS were not significantly correlated in any vegetation group. The SOS and GSL were significantly correlated in all six vegetation groups. The EOS and GSL showed a significant correlation in five vegetation groups with the exception of steppe. The SOS and MNDVI showed a significant correlation ($r = -0.591$, $p = 0.015$) in needleleaf forest. The EOS and MNDVI were significantly correlated in desert ($r = -0.664$, $p = 0.005$).

3.4. Relationships between phenology and climate

Generally, different vegetation groups were correlated with different climatic variables (Appendices, Tables A. 1–A. 4).

The SOS of needleleaf forest, scrub, and alpine vegetation was negatively correlated with temperature in May and April–May. The SOS of meadow showed a negative correlation with temperature in April and April–May. The SOS of steppe showed a negative correlation with temperature in April–May. The SOS of desert was negatively correlated with minimum annual temperature and that of the previous winter.

The EOS of needleleaf forest, steppe, and meadow showed a positive correlation with August precipitation and annual integrated index. The EOS of scrub was negatively correlated with July maximum temperature and positively correlated with July–August precipitation and minimum temperature. The EOS of desert showed a positive correlation with August precipitation, and a negative correlation with previous winter precipitation, and July and July–August temperature. The EOS of steppe and meadow showed a positive correlation with August precipitation. The EOS of alpine vegetation was positively correlated with May, April–May, and July–August precipitation and September temperature.

The GSL of needleleaf forest showed a positive correlation with May and April–May temperature. The GSL of scrub showed a positive correlation with annual precipitation and integrated index, and May and April–May temperature, and a negative correlation with July temperature. The GSL of desert was positively correlated with April and April–

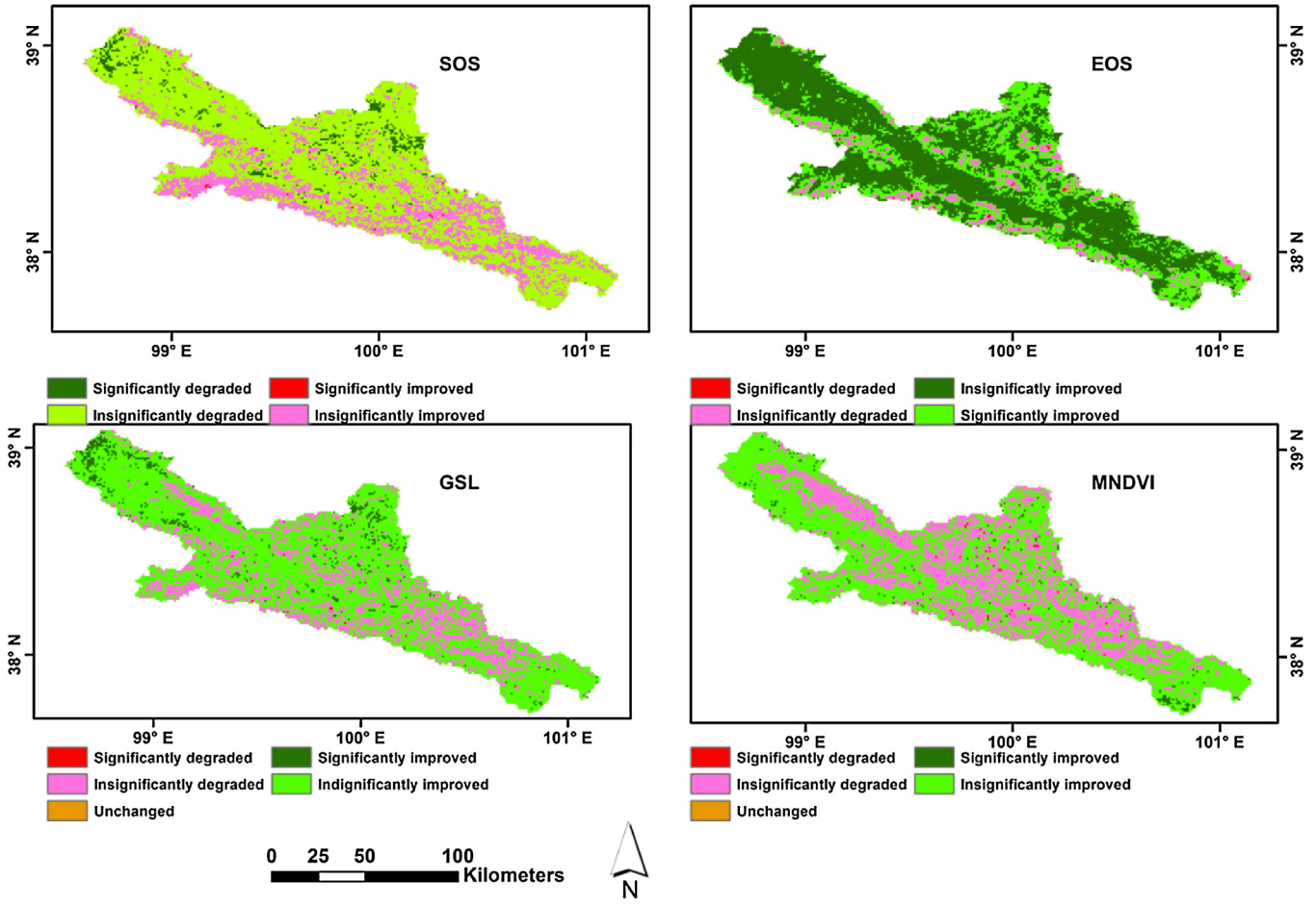

Fig. 4. Spatial pattern of 16-year phenology trends at the start of the growing season (SOS), end of the growing season (EOS), growing season length (GSL) and maximum normalized difference vegetation index (MNDVI) in the Heihe River headwaters. Theil–Sen values >0, equal to 0 and <0 were defined as "improved", "unchanged" and "degraded", respectively. Mann–Kendall test value >0.05 indicated a non-significant change and other value indicated a significant change.

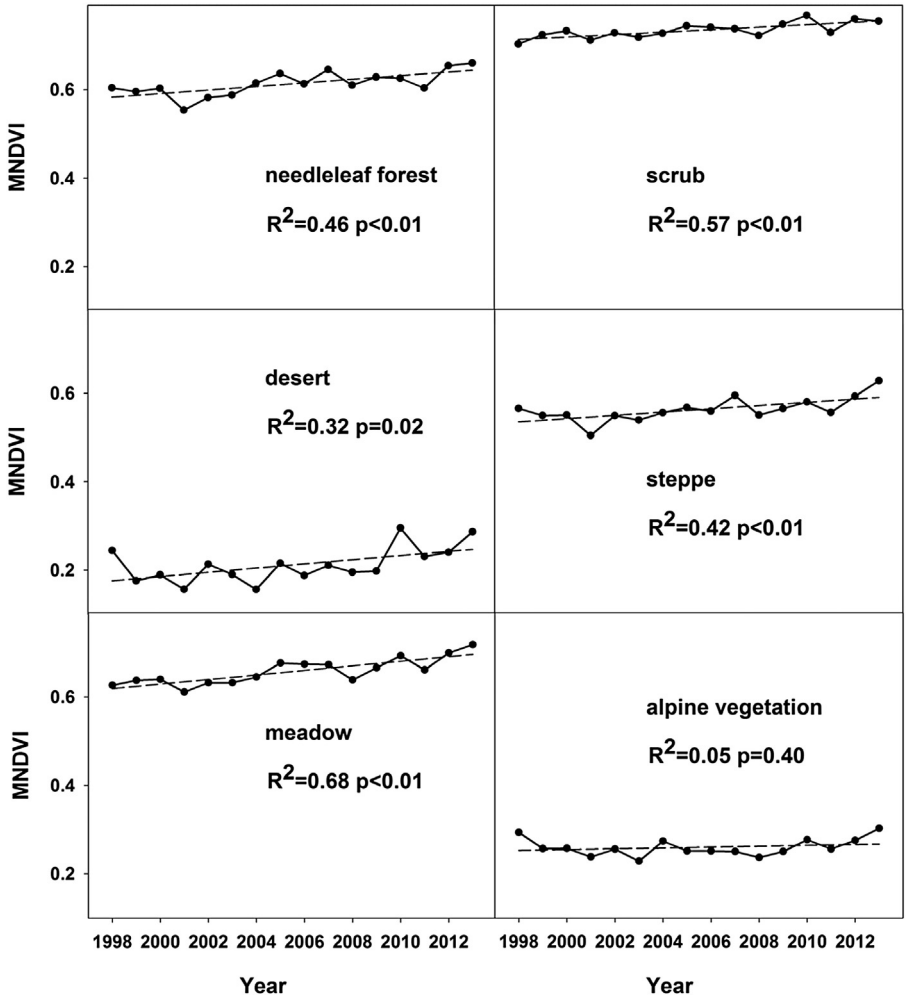

Fig. 5. Average maximum normalized difference vegetation index (MNDVI) with linear regression in six vegetation groups from 1998 to 2013 in the Heihe River headwaters. Description of the vegetation groups is presented in Table 1.

May minimum temperature. The GSL of steppe showed a positive correlation with April–May temperature and previous winter minimum temperature. The GSL of meadow was positively correlated with April and April–May temperature, annual and previous winter precipitation and minimum temperature, annual integrated index, and August precipitation. The GSL of alpine vegetation was positively correlated with annual and July–August precipitation, April–May mean temperature, and September maximum temperature, and negatively correlated with July and July–August maximum temperature.

The MNDVI of needleleaf forest showed a positive correlation with May and April–May temperature, and August and July–August minimum temperature. The MNDVI of scrub was positively correlated with annual, July, August, and July–August temperature. The MNDVI of desert showed a positive correlation with annual EAT and August and July–August temperature. The MNDVI of steppe was positively correlated with August temperature. The MNDVI of meadow was positively correlated with annual, August, and July–August temperature. The MNDVI of alpine vegetation showed a positive correlation with annual and June temperature.

3.5. Climate and grazing dynamics and relationships with phenological indices

Annual precipitation, annual mean temperature, maximum temperature, and minimum temperature of Qilian from 1998 to 2013 did not change significantly (Fig. 6). Meat and milk production from 1998 to 2013 increased significantly, especially from 2005 (Fig. 7). Among the phenological indices, only MNDVI showed a significant correlation with meat and milk production for scrub, steppe, and meadow (Table 3).

4. Discussion

4.1. Phenology of the vegetation groups

Previous research on the Tibetan Plateau has detected no significant trend in needleleaf forest phenology (Du et al., 2014), and no significant trend was detected for scrub phenological metrics, except for earlier SOS for scrub at some field stations (He et al., 2015), when Moderate Resolution Imaging Spectroradiometer (MODIS) NDVI data were used. Both of the above-mentioned studies were focused at the field-station level, whereas the current study was undertaken at the regional scale and a longer time series of remotely sensed data was used. These dissimilarities might account for the difference in results obtained. Piao et al. (2011) and Shen et al. (2014) also concluded that different remote sensing data sources and data time series may yield different results. Shen et al. (2014) observed no significant trend in the green-up date averaged over the entire Tibetan Plateau for the period 2000–2011, and a trend for increasing MNDVI on the Tibetan Plateau and Northern Hemisphere has been reported (Dai et al., 2010; Xu et al., 2012; Zhao et al., 2012; Wang et al., 2016b). Needleleaf forest, scrub, desert, steppe, and meadow showed similar phenological trends, whereas alpine

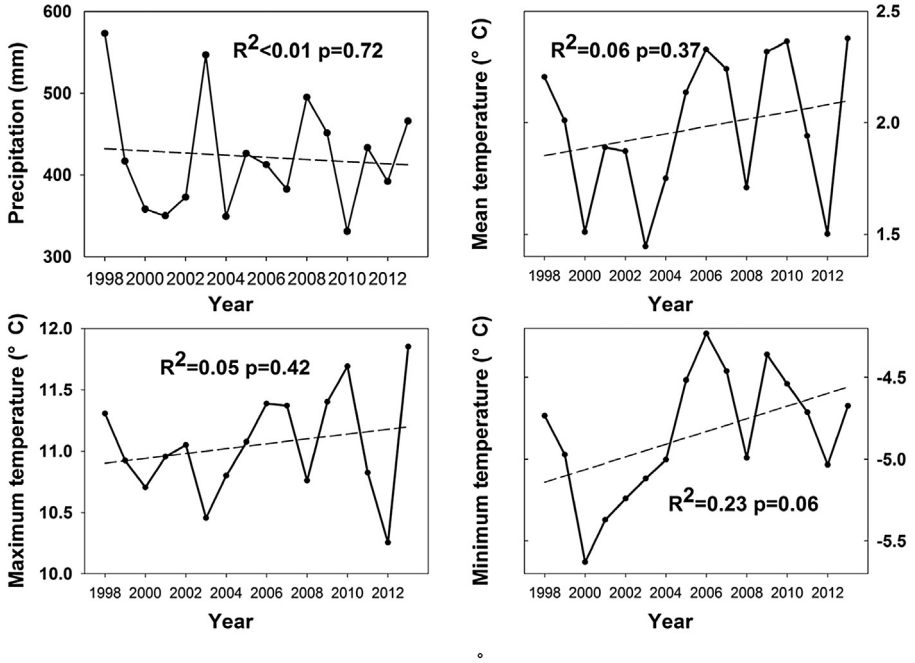

Fig. 6. Climate parameter dynamics with linear regression in Qilian County from 1998 to 2013.

vegetation showed different trends, possibly because at high elevations the environment shows greater changeability than at lower elevations. The rate of warming over the previous 15 years (1998–2012; 0.05 °C decade^{-1}) is significantly less than the rate calculated since 1951 (IPCC, 2013), thus phenological trends are similarly smaller and insignificant in recent years (Fu et al., 2015).

Cloud contamination is an obstacle to quantification of the phenology of alpine regions using optical satellite remote sensing data. In the Qilian Mountains, >40% of days are cloudy each year, and the degree of cloudiness is higher in the growing season (from June to September) (Du et al., 2014). The absence of field observations is a problem for the accuracy of satellite-derived phenology calibration, especially for rural areas such as the Tibetan Plateau (Zhao et al., 2012). Although the NDVI may be a good proxy for vegetation change, it does not directly reflect changes in species composition and community structure, and does not monitor processes such as shrub encroachment in grasslands (Zhao et al., 2012). Although satellite products can provide invaluable synoptic phenological information, they do not allow detailed evaluation of the variability in species responses (Julitta et al., 2014).

Previous studies have reported the correlation of SOS and EOS in North China (Wu et al., 2016) and northeastern United States (Keenan and Richardson, 2015). However, a similar relationship was not detected in the headwaters of the Heihe River Basin. Compared with the same species distributed in a warmer climate, the vegetation in the headwaters of the Heihe River Basin experiences a relatively short growing season, thus the biological character was not a major limiting factor for phenology.

4.2. Climate and phenology

Though the trends for changes in SOS, EOS, and GSL were not significant during the study period, these indices fluctuate in accordance with changes in the weather. Phenological metrics showed a significant correlation with the corresponding climatic variables in the month of occurrence or the former month and study period. Most phenological metrics were sensitive to temperature and a few were sensitive to precipitation or the integrated index. The SOS was significantly correlated with June temperature, and EOS was significantly correlated with September temperature for needleleaf forest (Du et al., 2014) and scrub (He et al., 2015). Differences in the remote sensing data, data time series, and spatial level of studies are likely to be the main reasons for differences in results. The EOS of temperate steppe in Northeast China is DOY 265–300, and the temperature and precipitation in August both affect the EOS (Yu et al., 2014). The GSL is mostly associated with SOS, hence the two indices showed similar correlations with climatic variables for needleleaf forest, scrub, steppe, and meadow in the headwaters of the Heihe River Basin, and the vegetation was limited mainly by the low temperature in the alpine region. To explore the correlation between climatic variables and phenological metrics, many time periods have been used, e.g., months (Du et al., 2014), double months

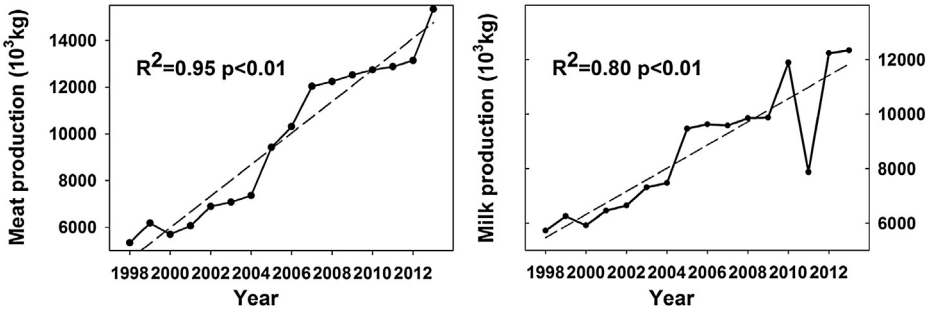

Fig. 7. Meat and milk production in Qilian County from 1998 to 2013.

Table 3
Correlation coefficients between grazing products and maximum normalized difference vegetation index (MNDVI) in the Heihe River headwaters.

	Scrub		Steppe		Meadow	
	r	p	r	p	r	p
Meat product	0.734	0.001	0.711	0.002	0.836	<0.001
Milk product	0.855	<0.001	0.734	0.001	0.899	<0.001

(He et al., 2015), seasons (Yu et al., 2014; Wang et al., 2016b), or different preseasons (30, 60, 90, 120, 150, and 180 days) (Cong et al., 2013). Climate data from the sparsely distributed climate stations adopted in previous studies might be insufficient to satisfactorily represent regional conditions, especially for high-elevation regions of the Tibetan Plateau. However, high-elevation climate data for a prolonged duration are rare, and climate trends often differ from nearby lower-elevation sites, which may lead to an unrealistic relationship between phenology and climate (Jin et al., 2013; Kimball et al., 2014).

Phenological metrics are more sensitive to inter-annual variation in preseason precipitation in arid areas than in more mesic areas (Shen et al., 2015a). Low temperatures leading to low evapotranspiration may be the cause of a non-significant correlation between precipitation and phenology in the present and previous studies on the Tibetan Plateau (Du et al., 2014). Among the temperature variables, minimum temperature, AT, and EAT showed stronger correlations with phenological metrics than that of mean temperature and maximum temperature, except that the SOS and EOS of alpine vegetation were more highly correlated with maximum temperature in May and September. The AT and EAT show better performance than mean temperature in correlation analyses and phenology models (Xin et al., 2015). Studies in Europe and the United States show that inter-annual anomalies of SOS during 1982–2011 are triggered by maximum temperature (daytime) more than by minimum temperature (nighttime) (Piao et al., 2015). Although a low temperature overnight may result in frost damage on the Tibetan Plateau (He et al., 2015), minimum temperature has a limited effect on SOS on the Tibetan Plateau. Alpine vegetation shows higher cold tolerance at night and is sensitive to maximum temperature. Recent research indicates that incorporating spatially explicit soil temperature and moisture information, instead of air temperature and precipitation, may improve phenology models (Jin et al., 2013). Although soil conditions play an important role in determining the timing of phenological events, the availability of soil data is limited, especially for rural areas.

4.3. Phenology and grazing

Variation in vegetation phenology affects vegetation activity and ecosystem functions. On the Tibetan Plateau, plant phenology may affect forage production on which livestock feed (Shen et al., 2015b). In the present study, SOS, EOS, and GSL were not correlated with grazing products because these phenological metrics did not change significantly in the study period, whereas meat and milk production increased dramatically (Fig. 7). The MNDVI was strongly correlated with net primary production (NPP) in the headwaters of the Heihe River Basin. The MNDVI increased significantly during the study period, and showed a strong correlation with grazing products in the main grazed vegetation groups (scrub, steppe, and meadow; Table 3). Thus, increasing NPP may improve grazing productivity. However, the increase in grazing productivity may be only partly explained by the increase in NPP. The dramatic increase in meat and milk production in Qilian County around 2005 coincided with technological changes in 2003–2005, such as rotational grazing, construction of a large number of warm houses for cattle, increased grazing productivity, and reduced winter mortality (Wang et al., 2016a). Rangeland degradation has been identified as a serious concern in alpine regions on the Tibetan Plateau (Harris et al., 2015), as a result of overgrazing and human activities (Li et al., 2016). Although the MNDVI increased during the study period, the *Stellera chamaejasme* community, which is a major toxic plant in alpine meadows of the Tibetan Plateau and serves as an indicator of grassland degradation, in some meadows attained about 60% coverage (Li et al., 2016). Limitation of cattle numbers is extremely important for regional vegetation protection and sustainable rangeland utilization.

5. Conclusions

At the regional scale, for the six vegetation groups, no significant trends in SOS, EOS, and GSL were detected, whereas the MNDVI of needleleaf forest, scrub, desert, steppe, and meadow increased significantly by 0.06, 0.045, 0.075, 0.06, and 0.075, respectively, in the Heihe River headwaters over the study period. The SOS and GSL were significantly correlated with temperature in May and April–May, whereas MNDVI was correlated with temperature in August and July–August. The EOS of the different vegetation groups was correlated with different climatic variables. The importance of the correlation of AT and EAT with phenological metrics was highlighted. No significant correlation between SOS and EOS was observed, thus the growing season limits were not a major limiting factor for phenology in the headwaters of the Heihe River. Although increased grazing productivity was correlated with increasing MNDVI, technological progress may have been a more important contributor to the increased productivity and moderate grazing is necessary for sustainable rangeland utilization.

Acknowledgements

This work was funded by National Natural Science Foundation of China [91225302].

Appendix A. Supplementary data

Supplementary data to this article can be found online at http://dx.doi.org/10.1016/j.scitotenv.2016.07.206.

References

Akritas, M.G., Murphy, S.A., Lavalley, M.P., 1995. The Theil-Sen estimator with doubly censored-data and applications to astronomy. J. Am. Stat. Assoc. 90, 170–177.
Bonan, G.B., 2008. Forests and climate change: forcings, feedbacks, and the climate benefits of forests. Science 320, 1444–1449.
Botzan, T.M., Mariño, M.A., Necula, A.I., 1998. Modified de Martonne aridity index: application to the Napa Basin, California. Phys. Geogr. 19, 55–70.
Brown, T.B., Hultine, K.R., Steltzer, H., Denny, E.G., Denslow, M.W., Granados, J., et al., 2016. Using phenocams to monitor our changing Earth: toward a global phenocam network. Front. Ecol. Environ. 14, 84–93.
Cheng, G., Li, X., Zhao, W., Xu, Z., Feng, Q., Xiao, S., et al., 2014. Integrated study of the water–ecosystem–economy in the Heihe River Basin. Nat. Sci. Rev. 1, 413–428.
Cong, N., Wang, T., Nan, H., Ma, Y., Wang, X., Myneni, R.B., et al., 2013. Changes in satellite-derived spring vegetation green-up date and its linkage to climate in China from 1982 to 2010: a multimethod analysis. Glob. Chang. Biol. 19, 881–891.
Dai, S.P., Zhang, B., Wang, H., Wang, Y.M., Li, D., Wang, X.M., 2010. Spatio temporal Variation of Vegetation NDVI in the Qilian Mountains during the Period from 1999 to 2007. Arid Zone Research, pp. 27,585–27,591 (in Chinese with English abstract).
Du, J., He, Z., Yang, J., Chen, L., Zhu, X., 2014. Detecting the effects of climate change on canopy phenology in coniferous forests in semi-arid mountain regions of China. Int. J. Remote Sens. 35, 6490–6507.
Editorial committee of vegetation map of China, CAS, 2007. The Vegetation Map of the People's Republic of China (1:1 000 000). Geological publishing house.
Fu, Y., Zhang, H.C., Dong, W.J., Yuan, W.P., 2014. Comparison of phenology models for predicting the onset of growing season over the Northern Hemisphere. PLoS One 9.
Fu, Y.S.H., Zhao, H.F., Piao, S.L., Peaucelle, M., Peng, S.S., Zhou, G.Y., et al., 2015. Declining global warming effects on the phenology of spring leaf unfolding. Nature 526, 104.
Gao, B., Qin, Y., Wang, Y.H., Yang, D.W., Zheng, Y.R., 2016. Modeling ecohydrological processes and spatial patterns in the Upper Heihe Basin in China. Forests 7, 21.

Ge, Q.S., Wang, H.J., Rutishauser, T., Dai, J.H., 2015. Phenological response to climate change in China: a meta-analysis. Glob. Chang. Biol. 21, 265–274.
Hamed, K.H., 2008. Trend detection in hydrologic data: the Mann–Kendall trend test under the scaling hypothesis. J. Hydrol. 349, 350–363.
Harris, R.B., Wang, W.Y., Badinqiuying, AT, S., DJ., B., 2015. Herbivory and competition of tibetan steppe vegetation in winter pasture: effects of livestock exclosure and plateau pika reduction. Plos One 10, 26.
He, Z.B., Du, J., Zhao, W.Z., Yang, J.J., Chen, L.F., Zhu, X., et al., 2015. Assessing temperature sensitivity of subalpine shrub phenology in semi-arid mountain regions of China. Agric. For. Meteorol. 213, 42–52.
IPCC, 2013. Carbon and other biogeochemical cycles. Climate Change 2013. The Physical Science Basis. Contribution of Working Group I to the Fifth Assessment Report of the Intergovernmental Panel on Climate Change. Cambridge University Press, Cambridge, United Kingdom and New York, NY, USA.
Jin, H.X., Eklundh, L., 2014. A physically based vegetation index for improved monitoring of plant phenology. Remote Sens. Environ. 152, 512–525.
Jin, Z., Zhuang, Q., He, J.-S., Luo, T., Shi, Y., 2013. Phenology shift from 1989 to 2008 on the Tibetan Plateau: an analysis with a process-based soil physical model and remote sensing data. Clim. Chang. 119, 435–449.
Jolly, W.M., Nemani, R., Running, S.W., 2005. A generalized, bioclimatic index to predict foliar phenology in response to climate. Glob. Chang. Biol. 11, 619–632.
Jonsson, P., Eklundh, L., 2004. TIMESAT - a program for analyzing time-series of satellite sensor data. Comput. Geosci. 30, 833–845.
Julitta, T., Cremonese, E., Migliavacca, M., Colombo, R., Galvagno, M., Siniscalco, C., et al., 2014. Using digital camera images to analyse snowmelt and phenology of a subalpine grassland. Agric. For. Meteorol. 198, 116–125.
Keenan, T.F., Richardson, A.D., 2015. The timing of autumn senescence is affected by the timing of spring phenology: implications for predictive models. Glob. Chang. Biol. 21, 2634–2641.
Kimball, K.D., Davis, M.L., Weihrauch, D.M., Murray, G.L.D., Rancourt, K., 2014. Limited alpine climatic warming and modeled phenology advancement for three alpine species in the northeast United States. Am. J. Bot. 101, 1437–1446.
Kira, T., 1991. Forest ecosystems of east and southeast Asia in a global perspective. Ecol. Res. 6 (2), 185–200.
Koerner, C., Basler, D., 2010. Phenology under global warming. Science 327, 1461–1462.
Lara, B., Gandini, M., 2016. Assessing the performance of smoothing functions to estimate land surface phenology on temperate grassland. Int. J. Remote Sens. 37, 1801–1813.
Leslie, H., 1967. Life Zone Ecology. Tropical Science Center, San José, Costa Rica.
Li, J.Z., Liu, Y.M., Mo, C.H., Wang, L., Pang, G.W., Cao, M.M., 2016. IKONOS image-based extraction of the distribution area of *Stellera chamaejasme* L. in Qilian county of Qinghai Province, China. Remote Sens. 8, 148.
Maisongrande, P., Duchemin, B., Dedieu, G., 2004. VEGETATION/SPOT: an operational mission for the Earth monitoring; presentation of new standard products. Int. J. Remote Sens. 25, 9–14.
Meng, M., Ni, J., Zhang, Z.G., 2004. Aridity index and its applications in geo-ecological study. Acta Phys. Sin. 28, 853–861 (in Chinese with English abstract).
Menzel, A., Fabian, P., 1999. Growing season extended in Europe. Nature 397, 659.
Pau, S., Wolkovich, E.M., Cook, B.I., Davies, T.J., Kraft, N.J.B., Bolmgren, K., et al., 2011. Predicting phenology by integrating ecology, evolution and climate science. Glob. Chang. Biol. 17, 3633–3643.
Penuelas, J., Rutishauser, T., Filella, I., 2009. Phenology feedbacks on climate change. Science 324, 887–888.
Piao, S., Cui, M., Chen, A., Wang, X., Ciais, P., Liu, J., et al., 2011. Altitude and temperature dependence of change in the spring vegetation green-up date from 1982 to 2006 in the Qinghai-Xizang Plateau. Agric. For. Meteorol. 151, 1599–1608.
Piao, S.L., Tan, J.G., Chen, A.P., Fu, Y.H., Ciais, P., Liu, Q., et al., 2015. Leaf onset in the northern hemisphere triggered by daytime temperature. Nat. Commun. 6, 8.
Qinghai Bureau of Statistics, 1998–2014. Qianghai Statistical Yearbook, Qinghai Bureau of Statistics.
Richardson, A.D., Anderson, R.S., Arain, M.A., Barr, A.G., Bohrer, G., Chen, G.S., et al., 2012. Terrestrial biosphere models need better representation of vegetation phenology: results from the North American Carbon Program Site Synthesis. Glob. Chang. Biol. 18, 566–584.
Richardson, A.D., Keenan, T.F., Migliavacca, M., Ryu, Y., Sonnentag, O., Toomey, M., 2013. Climate change, phenology, and phenological control of vegetation feedbacks to the climate system. Agric. For. Meteorol. 169, 156–173.
Shen, Y., Xiong, A., 2016. Validation and comparison of a new gauge-based precipitation analysis over mainland China. Int. J. Climatol. 36, 252–265.
Shen, M.G., Zhang, G.X., Cong, N., Wang, S.P., Kong, W.D., Piao, S.L., 2014. Increasing altitudinal gradient of spring vegetation phenology during the last decade on the Qinghai-Tibetan Plateau. Agric. For. Meteorol. 189, 71–80.
Shen, M.G., Piao, S.L., Cong, N., Zhang, G.X., Jassens, I.A., 2015a. Precipitation impacts on vegetation spring phenology on the Tibetan Plateau. Glob. Chang. Biol. 21, 3647–3656.
Shen, M.G., Piao, S.L., Dorji, T., Liu, Q., Cong, N., Chen, X.Q., et al., 2015b. Plant phenological responses to climate change on the Tibetan Plateau: research status and challenges. Nat. Sci. Rev. 2, 454–467.
Sun, J., Qin, X., Yang, J., 2015. The response of vegetation dynamics of the different alpine grassland types to temperature and precipitation on the Tibetan Plateau. Environ. Monit. Assess. 188, 1–11.
Wang, S., Wang, C., Duan, J., Zhu, X., Xu, G., Luo, C., et al., 2014. Timing and duration of phenological sequences of alpine plants along an elevation gradient on the Tibetan plateau. Agric. For. Meteorol. 189, 220–228.
Wang, J., Wang, Y., Li, S.C., Qin, D.H., 2016a. Climate adaptation, institutional change, and sustainable livelihoods of herder communities in northern Tibet. Ecol. Soc. 21, 5.
Wang, Y.L., Gao, Q., Liu, T., Tian, Y.Q., Yu, M., 2016b. The greenness of major shrublands in China increased from 2001 to 2013. Remote Sens. 8, 121.
Wolkovich, E.M., Cook, B.I., Allen, J.M., Crimmins, T.M., Betancourt, J.L., Travers, S.E., et al., 2012. Warming experiments underpredict plant phenological responses to climate change. Nature 485, 494–497.
Wu, C.Y., Hou, X.H., Peng, D.L., Gonsamo, A., Xu, S.G., 2016. Land surface phenology of China's temperate ecosystems over 1999–2013: spatial-temporal patterns, interaction effects, covariation with climate and implications for productivity. Agric. For. Meteorol. 216, 177–187.
Xin, Q.C., Broich, M., Zhu, P., Gong, P., 2015. Modeling grassland spring onset across the Western United States using climate variables and MODIS-derived phenology metrics. Remote Sens. Environ. 161, 63–77.
Xu, H.J., Yang, T.B., Zeng, B., 2012. Spatial-temporal changes of vegetation in Qilian Mountains from 2000 to 2010 based on MODIS NDVI data and its affecting factors. J. Arid Land Res. Environ. 26, 87–91 (in Chinese with English abstract).
Yang, D., Li, C., Hu, H., Lei, Z., Yang, S., Kusuda, T., et al., 2004. Analysis of water resources variability in the Yellow River of China during the last half century using historical data. Water Resour. Res. 40.
Yu, X.F., Wang, Q.K., Yan, H.M., Wang, Y., KG, W., DF, Z., et al., 2014. Forest Phenology Dynamics and Its Responses to Meteorological Variations in Northeast China. Advances in Meteorology.
Zhang, G., Zhang, Y., Dong, J., Xiao, X., 2013. Green-up dates in the Tibetan Plateau have continuously advanced from 1982 to 2011. Proc. Natl. Acad. Sci. U. S. A. 110, 4309–4314.
Zhao, X., Zhou, D.J., Fang, J.Y., 2012. Satellite-based studies on large-scale vegetation changes in China. J. Integr. Plant Biol. 54, 713–728.
Zhou, H.K., Yao, B.Q., Xu, W.X., Ye, X., Fu, J.J., Jin, Y.X., et al., 2014. Field evidence for earlier leaf-out dates in alpine grassland on the eastern Tibetan Plateau from 1990 to 2006. Biol. Lett. 10.